Supplementary Information: Real-time computed optical interferometric tomography

Adeel Ahmad*[,1,2], Nathan D. Shemonski*[,1,2], Steven G. Adie[1,2], Hee-Seok Kim[1], Wen-Mei W. Hwu[1], P. Scott Carney[1,2] and Stephen A. Boppart[†,1,2,3]

[1]*Beckman Institute for Advanced Science and Technology, University of Illinois at Urbana-Champaign*
[2]*Department of Electrical and Computer Engineering, University of Illinois at Urbana-Champaign*
[3]*Departments of Bioengineering and Internal Medicine, University of Illinois at Urbana-Champaign*
**Equally contributing authors,* [†]*boppart@illinois.edu*

Decomposition of Fourier Space Resampling

Notation here is consistent with previous ISAM derivations[1,2] except that q_z is used instead of β. Let $\tilde{S}(\mathbf{r}_\parallel, k)$ be the measured SD-OCT signal after linearization in wavenumber with $\mathbf{r}_\parallel$ as the transverse spatial dimensions, $\mathbf{q} = (q_x, q_y)$ the transverse spatial frequencies, q_z the axial spatial frequency, and k the wavenumber. We desire to recover the scattering potential, $\eta(\mathbf{r}_\parallel, z)$, from $\tilde{S}$, which after proper approximations [1], is related as follows

$$\tilde{\tilde{\tilde{S}}}(\mathbf{q},k) = A(k)\left(\frac{i2\pi^2}{k_z(\mathbf{q},k)}\frac{k^2}{\alpha^2}\mathrm{e}^{-\frac{\alpha^2|\mathbf{q}|^2}{4k^2}}\right)\tilde{\tilde{\tilde{\eta}}}(\mathbf{q},-2k_z(\mathbf{q}/2,k)) \tag{1}$$

where $k_z(\mathbf{q},k) = \sqrt{k^2 - |\mathbf{q}|^2}$, $A(k)$ is the square root of the power spectral density, $\alpha = \pi / \mathrm{NA}$, and each $\tilde{}$ (tilde) represents a Fourier transform over one spatial dimension. To properly invert (1), regularization (e.g. Tikhonov regularization) must be performed, though no significant loss of information is seen[2] by approximating $\eta(\mathbf{r}_\parallel, z)$ as

$$\eta(\mathbf{r}_\parallel, z) \approx \mathcal{F}^{-1}_{\mathbf{q}\to\mathbf{r}_\parallel, q_z\to z}\left\{\tilde{\tilde{\tilde{S}}}(\mathbf{q},k)\Big|_{k=\frac{1}{2}\sqrt{q_z^2+|\mathbf{q}|^2}}\right\} \tag{2}$$

where $\mathcal{F}^{-1}$ is an inverse Fourier transform. Without regularization, the final reconstruction is less quantitative, but more suitable for real-time implementations.

Notice that one great difficulty with implementing a Fourier space resampling such as in (2) for real-time applications is that most of the processing cannot be completed until the full volume has been acquired. Thus, if implemented directly from (2), multiple volumes of data must be held in onboard memory - one volume would complete its ISAM reconstruction as the next volume is acquired.

We can mitigate this memory requirement by decomposing the 3-D resampling problem into two separate 2-D resampling steps, each with lower memory requirements. First, we rewrite the resampling function as

$$k = \frac{1}{2}\sqrt{{q_z}^2 + |\mathbf{q}|^2} = \frac{1}{2}\sqrt{{q_z}^2 + q_x^2 + q_y^2} = \frac{1}{2}\sqrt{\left(2k_{1/2}(q_z, q_y)\right)^2 + q_x^2} \tag{3}$$

Where q_x and q_y are Fourier variables for the two transverse dimensions and $k_{1/2}(q_z, q_y) = \frac{1}{2}\sqrt{{q_z}^2 + q_y^2}$ is an intermediate function which allows us to properly decompose the 3-D ISAM reconstruction into two sets of 2-D reconstructions. We then let $q_{z,1/2} = 2k_{1/2}$ and perform an ISAM reconstruction along the fast-axis as

$$\eta_{\text{fast}}(x, y, z_{1/2}) \approx \mathcal{F}^{-1}_{q_x \to x, q_{z,1/2} \to z_{1/2}} \left\{ \tilde{\tilde{S}}(q_x, y, k)\Big|_{k=\frac{1}{2}\sqrt{q_{z,1/2}^2 + q_x^2}} \right\} \tag{4}$$

As (4) can be computed independently for each fast-axis frame, this reconstruction is performed efficiently on a frame-by-frame basis along with standard OCT processing to be displayed immediately. Once an entire volume is acquired and processed along the fast-axis, the full 3-D ISAM reconstruction is then efficiently completed by

$$\eta(x,y,z) = \mathcal{F}^{-1}_{q_y \to y, q_z \to z} \left\{ \tilde{\tilde{\eta}}_{\text{fast}}(x, q_y, k_{1/2}) \Big|_{k_{1/2} = \frac{1}{2}\sqrt{q_z^2 + q_y^2}} \right\} \tag{5}$$

Single GPU Implementation

The real-time 3-D ISAM reconstruction was done on the GPU based on equations (4) and (5) by performing two orthogonal 2-D ISAM reconstructions, one along the fast-axis frames as the data is being acquired and the other along orthogonal planes of the 2-D ISAM reconstructed fast-axis dataset after one volume latency (Fig. S1 and S2).

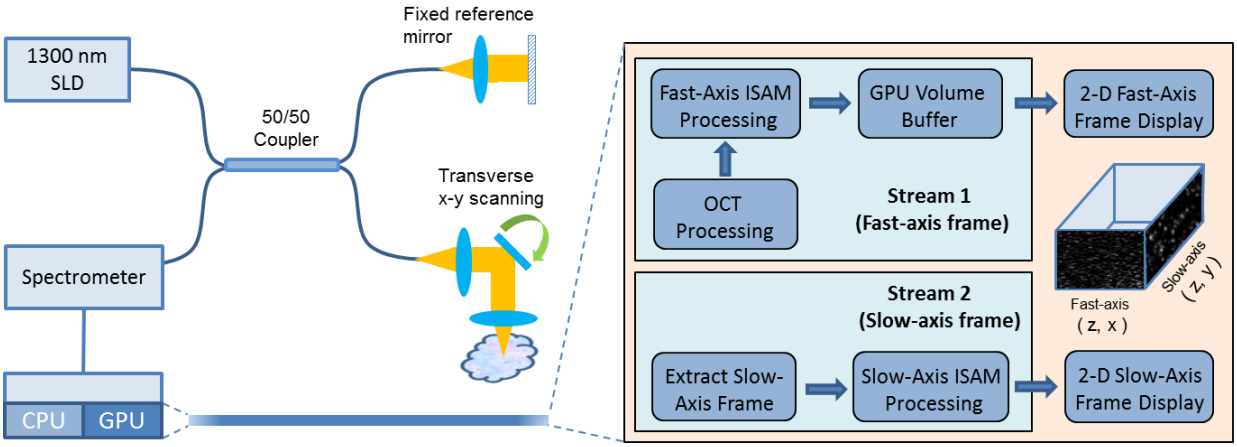

Figure S1: System diagram. The experimental setup showing the spectral-domain 1300 nm OCT system with an overview of the GPU implementation of real-time 3-D ISAM.

The background spectrum, the resampling indices for linearization in wavenumber, and ISAM resampling indices are pre-calculated in the initialization phase. The standard OCT processing steps of background subtraction, cubic B-spline interpolation for linearization in wavenumber *k*, and a real-to-complex (R2C) Fourier transform were performed on each A-scan. The signal processing steps for 2-D ISAM have been previously described[2]. Briefly, after the standard OCT processing, the cross-sectional images are circularly shifted to move the focus to zero optical path length difference, followed by a 2-D complex-to-complex (C2C) Fourier transform and ISAM resampling. Notice from (4) and (5), with proper spatial sampling, the same resampling indices can be used for both fast-axis and slow-axis Fourier space resampling. Finally, a (C2C) 2-D FFT brings the resampled data into the spatial domain, and the focus is

shifted back to its original location. The absolute value and gamma correction were applied on the data for display purposes, while the complex-valued data was transferred to a buffer on the GPU large enough to hold an entire volume for processing along the slow-axis.

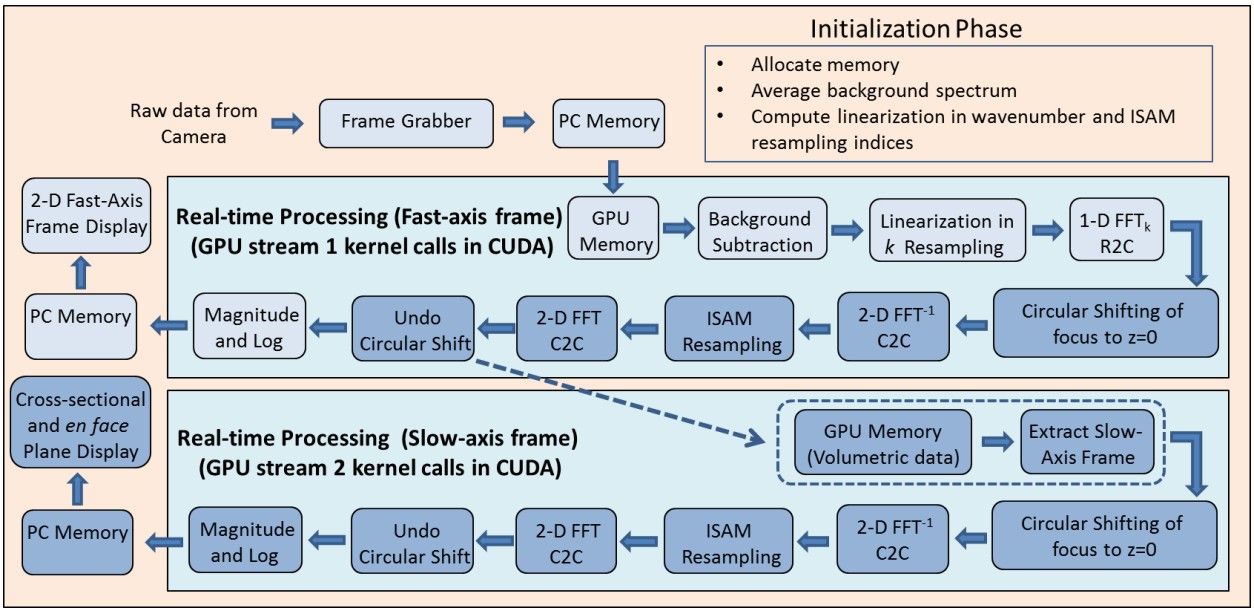

Figure S2: Flow chart for ISAM implementation on the GPU. The dark blue blocks indicate the additional steps required for ISAM processing. The GPU kernels along the fast- and slow-axes are executed on separate GPU threads enabling the GPU to schedule the kernels independently. The dashed rectangle denotes that these blocks are all performed in a single GPU kernel call. FFT (Fast Fourier Transform), R2C (Real-to-Complex), C2C (Complex-to-Complex), CUDA (Compute Unified Device Architecture).

Alternate Implementation

Throughout this document, ISAM was implemented on a GPU by allocating a single memory buffer capable of holding a full complex volume on the GPU. For situations where a full volume cannot be held on the GPU, the Fourier space decomposition also allows for an alternate implementation where the OCT/ISAM data is stored in CPU memory. Each time a new fast-axis frame is acquired and transferred to the GPU for OCT and 2-D ISAM processing instead of storing this frame on the GPU, it can be immediately transferred to the CPU for storage. At the same time, a slow-axis frame from the previously acquired volume can be transferred from CPU memory to the GPU for 2-D ISAM processing to complete the full 3-D reconstruction. Although this implementation suffers from more data transfers between the

CPU and GPU, if these transfers can be overlapped with data processing, much of the overhead can be hidden and camera-limited processing rates may still be possible.

Validation of real-time ISAM with a tissue mimicking phantom

A tissue mimicking phantom consisting of titanium (IV) oxide particles (< 5 μm) embedded in a silicone gel was used to quantitatively evaluate the reconstruction quality. The volumetric dataset (512 x 810 x 810) was acquired at 95 frames per second with the focus placed approximately 1 mm deep within the sample. Representative OCT-, 2-D ISAM-, and 3-D ISAM-processed *en face* planes 900 μm above the focus are shown in Fig. S3 while the Supplementary Video 1 shows a fly-through of the *en face* planes at different depths within the sample. The degradation of lateral resolution in OCT and the impact of ISAM resampling are clearly evident at the planes away from the focus. 2-D ISAM processing applied on the cross-sectional fast-axis frames results in narrowing of the point spread functions (PSFs) albeit only along the fast scanning direction. Subsequent ISAM processing along the slow-axis frames results in isotropic PSFs as would be expected from sub-resolution particles. These improvements were quantified by evaluating the full width half maximum values of the lateral PSFs at each depth by a method described previously[3]. Depth invariant transverse resolution both along the fast- and slow-axes was achieved after applying 3-D ISAM, as can be seen in Fig. S3. We also show a quality comparison between the real-time GPU reconstruction and 3-D ISAM post-processed in MATLAB. At high image acquisition speeds, we found that several computational steps, such as axial and lateral phase correction, were unnecessary. Furthermore, to minimize the processing time, data upsampling, dispersion compensation, and centering of the transverse bandwidth were not performed. To validate the decomposition of 3-D ISAM resampling, we post-processed the raw data based on equation (2) in MATLAB using double precision operations and also incorporated the above mentioned additional processing steps. Our results qualitatively and quantitatively show that, even for a high-NA OCT system, there was no degradation in reconstruction quality between the real-time GPU and MATLAB post-processed datasets.

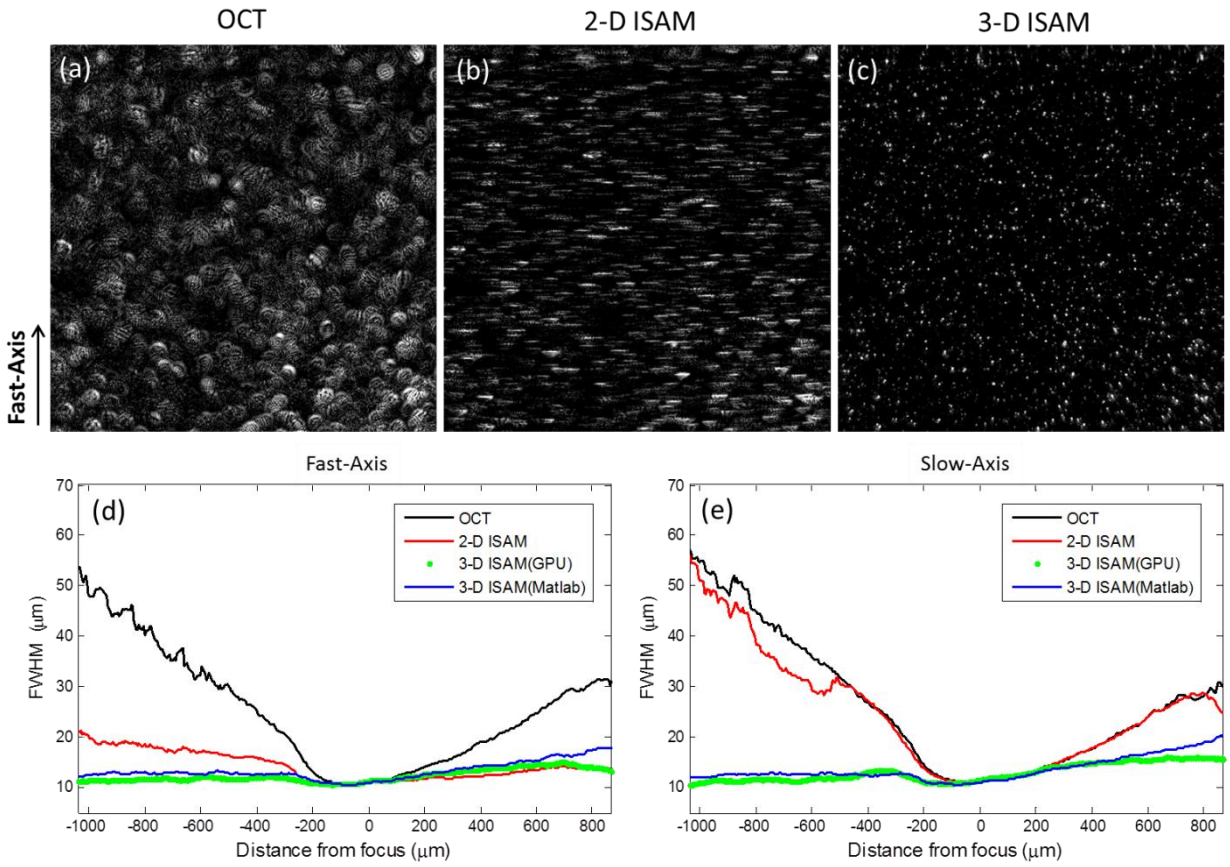

Figure S3: Results from tissue phantoms containing titanium (IV) oxide scattering particles. *En face* planes 900 μm above the focus for (a) OCT (b) 2-D ISAM processed along the fast-axis (c) 3-D ISAM reconstruction. Full-width-half-maximum (FWHM) of the point spread functions as a function of depth along the (d) fast-axis and (e) slow-axis for OCT, 2-D ISAM, GPU processed 3-D ISAM and MATLAB processed 3-D ISAM.

References

1 Ralston, T. S., Marks, D. L., Carney, P. S. & Boppart, S. A. Interferometric synthetic aperture microscopy. *Nature Phys.* **3**, 129-134 (2007).

2 Ralston, T. S., Marks, D. L., Carney, P. S. & Boppart, S. A. Real-time interferometric synthetic aperture microscopy. *Opt. Express* **16**, 2555-2569 (2008).

3 Ralston, T. S., Adie, S. G., Marks, D. L., Boppart, S. A. & Carney, P. S. Cross-validation of interferometric synthetic aperture microscopy and optical coherence tomography. *Opt. Lett.* **35**, 1683-1685 (2010).